



Synthesis and activity mechanism of some novel 2-substituted benzothiazoles as hGSTP1-1 enzyme inhibitors

K. Bolelli, Y. Musdal, E. Aki-Yalcin, B. Mannervik & I. Yalcin

To cite this article: K. Bolelli, Y. Musdal, E. Aki-Yalcin, B. Mannervik & I. Yalcin (2017) Synthesis and activity mechanism of some novel 2-substituted benzothiazoles as hGSTP1-1 enzyme inhibitors, SAR and QSAR in Environmental Research, 28:11, 927-940, DOI: 10.1080/1062936X.2017.1402820

To link to this article: <https://doi.org/10.1080/1062936X.2017.1402820>



Published online: 05 Dec 2017.



Submit your article to this journal [↗](#)



Article views: 5



View related articles [↗](#)



View Crossmark data [↗](#)



Synthesis and activity mechanism of some novel 2-substituted benzothiazoles as hGSTP1-1 enzyme inhibitors[§]

K. Bolelli^a, Y. Musdal^b, E. Aki-Yalcin^a, B. Mannervik^b and I. Yalcin^a

^aDepartment of Pharmaceutical Chemistry, Faculty of Pharmacy, Ankara University, Ankara, Turkey;

^bDepartment of Neurochemistry, Stockholm University, Stockholm, Sweden

ABSTRACT

Human GSTP1-1 is one of the most important proteins, which overexpresses in a large number of human tumours and is involved in the development of resistance to several anticancer drugs. So, it has become an important target in cancer treatment. In this study, 12 benzothiazole derivatives were synthesized and screened for their in vitro inhibitory activity for hGSTP1-1. Among these compounds, two of them (compounds #2 and #5) have been found to be the leads when compared with the reference drug etoposide. In order to analyse the structure–activity relationships (SARs) and to investigate the binding side interactions of the observed lead compounds, a HipHop pharmacophore model was generated and the molecular docking studies were performed by using CDocker method. In conclusion, it is observed that the lead compounds #2 and #5 possessed inhibitory activity on the hGSTP1-1 by binding to the H-site as a substrate in which the *para* position of the phenyl ring of the benzamide moiety on the benzothiazole ring is important. Substitution at this position with a hydrophobic group that reduces the electron density at the phenyl ring is required for the interaction with the H side active residue Tyr108.

ARTICLE HISTORY

Received 6 November 2017
Accepted 6 November 2017

KEYWORDS

Anticancer; benzothiazole; docking; hGSTP1-1; GSTs; pharmacophore

Introduction

One of the major problems with cancer treatment is multidrug resistance, depending on overexpression of glutathione transferases (GSTs). The GSTs are a family of widely distributed Phase II detoxification enzymes that catalyse the conjugation of the tripeptide glutathione (GSH) to electrophiles, resulting in the formation of the corresponding GSH conjugates [1–6]. Human GST P1-1 (hGSTP1-1) is the most prevalent isoform and is frequently overexpressed in human tumours, including carcinoma of the lung, kidney, ovary, colon, pancreas, stomach and oesophagus. These may play a role in resistance to anticancer drugs such as etoposide or doxorubicin, especially if associated with multidrug resistance proteins (MRP1, MRP2) [7,8]. Additionally, they can inhibit the part of the apoptosis control system, Jun N-terminal kinase and defend tumour cells by direct detoxification of anticancer drugs in this way [9,10].

CONTACT I. Yalcin  yalcin@ankara.edu.tr

[§]Presented at the 9th International Symposium on Computational Methods in Toxicology and Pharmacology Integrating Internet Resources, CMTPI-2017, 27–30 October 2017, Goa, India.

According to all these data, hGSTP1-1 can be a promising target for cancer treatment and considerable efforts have been undertaken to find specific inhibitors of hGSTP1-1.

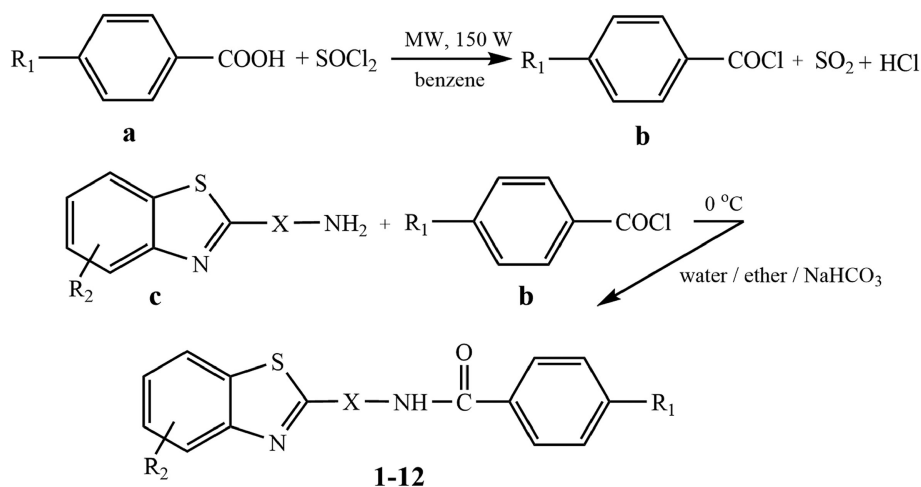
Ethacrynic acid (EA), which is an approved drug, inhibits hGSTP1-1 by binding directly to the substrate binding site (H site) of the enzyme, as well as by depleting its cofactor (GSH) via conjugation to the thiol group of GSH [11,12]. Recently, some heterocyclic compounds such as di-substituted benzoxazole derivatives were reported as hGSTP1-1 inhibitors [13–15].

Herein, we have described the synthesis of a series of 2-substituted benzothiazole derivatives and investigated their inhibitory activities towards hGSTP1-1. According to *in vitro* inhibitory activity results, two of the tested compounds (compounds #2 and #5) showed inhibitory activity potency similar to the reference drug, EA. In order to perform the structure–activity relationships and describe the binding site features of these lead benzothiazole derivatives on hGSTP1-1, pharmacophore analyses (HipHop) and molecular docking (CDocker) studies were performed by using Discovery Studio (DS) 3.5 software [16].

Methods

Compounds

In this study, 12 derivatives of substituted benzothiazoles [2-(4'-bromo/methyl/nitro benzamido)-4/6-substituted benzothiazoles and 2-(4'-bromo-*N'*-benzhydrazido) benzothiazole] (compounds #1–12) were synthesized, with five of them (compounds #5–7, 9 and 11) being original. Structures of the synthesized benzothiazoles are presented in Figure 1. The synthesis and characteristics of compounds are described below.



X: -; -NH-; **R1:** -H; -Br; -CH₃; -NO₂; **R2:** -H; 4-CH₃; 6-F; 6-CH₃

Figure 1. The synthesis of the tested compounds.

Synthesis

For reaching the targeted compounds, 1 mmol of appropriate carboxylic acid (4-bromo/methyl/nitro benzoic acid or non-substituted benzoic acid) (a), was exposed to a microwave energy of 150 W at a pressure of 250 psi and a temperature of 150°C for 10 min in the mixture of 0.3 ml thionyl chloride and 0.5 ml benzene. Then excess thionyl chloride was removed *in vacuo*. The residue, acyl chloride (b), was dissolved in anhydrous diethyl ether (1 ml) and solution added during 1 h to a stirred, ice-cold mixture of 2-amino-4/6-substituted benzothiazole or 2-hydrazinobenzothiazole (1 mmol) (c), sodium bicarbonate (2 mmol), diethyl ether (1 ml) and water (1 ml) [17]. The mixture was stirred overnight at room temperature and then filtered. Then, the precipitate was washed with water, 2N hydrochloric acid and water. Ethanol was used for recrystallization and crystals were dried *in vacuo*. Hence, the final benzothiazole derivatives (Compounds #1–12) were yielded (Figure 1).

Instruments

The chemicals were purchased from the commercial vendors and were used without purification. The reaction of chlorination was carried out by using CEM Discovery SP microwave apparatus. The reactions were monitored and the purity of the products was checked by thin layer chromatography (TLC). SilicaGel 60 HF₂₅₄ chromatoplates (0.3 mm) were used for TLC and the solvent systems were *n*-hexan:ethyl acetate (3:1) for 2-(4'-bromo/methyl/nitrobenzamido-4/6-substituted benzothiazole (#1–11) and *n*-hexan:ethyl acetate (1:1) for 2-(4'-bromo-*N'*-benzhydrazido)benzothiazole (#12). Melting points were taken on a Buchi Melting Point B-540 capillary apparatus and were uncorrected. ¹H-NMR and ¹³C-NMR spectra were obtained with a Varian Mercury 400 High Performance Digital FT-NMR-400 MHz spectrometer in dimethylsulphoxide-*d*₆ (DMSO-*d*₆); tetramethylsilane (TMS) was used as an internal standard. Elemental analyses were carried out with CHNS-932 (LECO) apparatus. The results (C, H, N) were within ±0.4% of the calculated values. Mass analysis was obtained by Waters 2695 Alliance Micromass ZQ LC-MS using the Electrospray Ionization (ESI) method.

In the enzyme studies, Mettler Toledo pH meter apparatus and the Shimadzu UV-2501 PC Spectrometer were used.

Characteristics of the compounds

2-Benzamidobenzothiazole (compound #1) [18]. Yield: 53% mp 188–189°C. ¹H NMR (DMSO-*d*₆, 400 MHz) δ (ppm): 7.33–7.37 (m, 1H, H-6), 7.46–7.50 (m, 1H, H-5), 7.56–7.60 (m, 2H, H-3', H-5'), 7.66–7.70 (m, 1H, H-4'), 7.80 (d, *J* = 8.4 Hz, 1H, H-7), 8.03 (d, *J* = 7.6 Hz, 1H, H-4), 8.16 (d, *J* = 7.2 Hz, 2H, H-2', H-6'), 12.91 (s, 1H, NH); ¹³C NMR (DMSO-*d*₆, 100 MHz) δ (ppm): 120.31, 121.73, 123.67, 126.17, 128.31, 128.63, 131.45, 132.86, 148.31, 158.86, 165.96; ESIMS *m/z* 255.18 (M⁺+H, 100%). Analytically Calculated (Anal. Calcd.) (%) for C₁₄H₁₀N₂OS: C, 66.12; H, 3.964; N, 11.016; S, 12.609. Found: C, 66.10; H, 3.736; N, 11.280; S, 12.670.

2-(4'-Bromobenzamido)benzothiazole (compound #2) [19]. Yield: 51% mp 239–240°C. ¹H NMR (DMSO-*d*₆, 400 MHz) δ (ppm): 7.34 (t, 1H, H-6), 7.45–7.49 (m, 1H, H-5), 7.77 (d, *J* = 9.2 Hz, 3H, H-3', H-5', H-7), 8.01 (d, *J* = 8.4 Hz, 1H, H-4), 8.07 (d, *J* = 8.0 Hz, 2H, H-2', H-6'), 12.99 (s, 1H, NH); ¹³C NMR (DMSO-*d*₆, 100 MHz) δ (ppm): 120.27, 121.78, 123.74, 126.23, 126.82, 130.38, 131.23, 131.66; ESIMS *m/z* 333.24 (M⁺+H, 100%), 335.24 (M⁺+H+2, 83%). Anal. Calcd. (%) for C₁₄H₉BrN₂OS: C, 50.47; H, 2.723; N, 8.407; S, 9.624. Found: C, 50.01; H, 2.657; N, 8.746; S, 9.631.

2-(4'-Methylbenzamido)benzothiazole (compound #3) [19,20]. Yield: 27% mp 188–189°C. ^1H NMR (DMSO- d_6 , 400 MHz) δ (ppm): 2.38 (s, 3H, CH_3), 7.20 (d, $J = 8.4$ Hz, 2H, H-3', H-5'), 7.26–7.29 (m, 3H, H-5, H-6, H-7), 7.83–7.86 (m, 1H, H-4), 7.89 (d, $J = 8.0$ Hz, 2H, H-2', H-6'), NH proton was not monitored; ^{13}C NMR (DMSO- d_6 , 100 MHz) δ (ppm): 21.58, 120.69, 121.34, 123.92, 126.01, 127.92, 129.15, 129.68, 131.91, 143.94, 147.75, 159.74, 165.78; ESIMS m/z 269.33 ($\text{M}^+\text{+H}$, 100%). Anal. Calcd. (%) for $\text{C}_{15}\text{H}_{12}\text{N}_2\text{OS}$: C, 67.14; H, 4.508; N, 10.44; S, 11.95. Found: C, 66.86; H, 4.245; N, 10.61; S, 11.82.

2-(4'-Nitrobenzamido)benzothiazole (compound #4) [19,20]. Yield: 42% mp 295–296°C (No information about melting point in the references). ^1H NMR (DMSO- d_6 , 400 MHz) δ (ppm): 7.34–7.38 (m, 1H, H-6), 7.46–7.50 (m, 1H, H-5), 7.78 (d, $J = 7.6$ Hz, 1H, H-7), 8.02 (d, $J = 8.0$ Hz, 1H, H-4), 8.33–8.39 (m, 4H, H-2', H-3', H-5', H-6'), 13.25 (s, 1H, NH); ^{13}C NMR (DMSO- d_6 , 100 MHz) δ (ppm): 118.83, 119.73, 121.86, 123.53, 123.84, 126.32, 129.84, 131.06, 137.99, 144.91, 149.69, 152.77; ESIMS m/z 300.21 ($\text{M}^+\text{+H}$, 100%). Anal. Calcd. (%) for $\text{C}_{14}\text{H}_9\text{N}_3\text{O}_3\text{S}$: C, 56.18; H, 3.031; N, 14.039; S, 10.714. Found: C, 55.83; H, 3.238; N, 14.08; S, 10.73.

2-(4'-Bromobenzamido)-4-methylbenzothiazole (compound #5). Yield: 55% mp 190–191°C (Decomposed at 171–172°C). ^1H NMR (DMSO- d_6 , 400 MHz) δ (ppm): 2.62 (s, 3H, CH_3), 7.21–7.29 (m, 2H, H-5, H-6), 7.77 (d, $J = 8.8$ Hz, 2H, H-3', H-5'), 7.82 (d, $J = 7.6$ Hz, 1H, H-7), 8.08 (d, $J = 8.4$ Hz, 2H, H-2', H-6'), 12.98 (s, 1H, NH); ^{13}C NMR (DMSO- d_6 , 100 MHz) δ (ppm): 18.07, 119.06, 123.68, 126.70, 126.77, 129.94, 130.43, 131.13, 131.61; ESIMS m/z 347.31 ($\text{M}^+\text{+H}$, 100%), 349.25 ($\text{M}^+\text{+H}+2$, 96%). Anal. Calcd. (%) for $\text{C}_{15}\text{H}_{11}\text{BrN}_2\text{OS} - 1.1\text{HOH}$: C, 49.08; H, 3.625; N, 7.632; S, 8.736. Found: C, 48.79; H, 3.824; N, 8.023; S, 8.791.

2-(4'-Nitrobenzamido)-4-methylbenzothiazole (compound #6). Yield: 71% mp 237–238°C. ^1H NMR (DMSO- d_6 , 400 MHz) δ (ppm): 2.61 (s, 3H, CH_3), 7.21–7.28 (m, 2H, H-5, H-6), 7.82 (d, $J = 8.0$ Hz, 1H, H-7), 8.32–8.36 (m, 4H, H-2', H-3', H-5', H-6'), 13.23 (s, 1H, NH); ^{13}C NMR (DMSO- d_6 , 100 MHz) δ (ppm): 17.96, 119.10, 123.48, 123.79, 126.72, 129.88, 149.65; ESIMS m/z 314.20 ($\text{M}^+\text{+H}$, 100%). Anal. Calcd. (%) for $\text{C}_{15}\text{H}_{11}\text{N}_3\text{O}_3\text{S} - 1.1\text{HOH}$: C, 57.5; H, 3.539; N, 13.411; S, 10.234. Found: C, 57.35; H, 3.581; N, 13.27; S, 9.985.

2-(4'-Bromobenzamido)-6-fluorobenzothiazole (compound #7). Yield: 47% mp 271–272°C. ^1H NMR (DMSO- d_6 , 400 MHz) δ (ppm): 7.29–7.34 (m, 1H, H-5), 7.76–7.80 (m, 3H, H-3', H-5', H-7), 7.92 (dd, $J = 2.4$ Hz and $J = 8.4$ Hz, 1H, H-4), 8.06 (d, $J = 8.8$ Hz, 2H, H-2', H-6'), 13.00 (s, 1H, NH); ^{13}C NMR (DMSO- d_6 , 100 MHz) δ (ppm): 108.18 (d, $J_{\text{C-F}} = 27$ Hz), 114.33 (d, $J_{\text{C-F}} = 24$ Hz), 121.49, 126.89, 130.36, 130.99, 132.69, 145.01, 158.76 (d, $J_{\text{C-F}} = 239$ Hz), 165.20; ESIMS m/z 351.29 ($\text{M}^+\text{+H}$, 100%), 353.34 ($\text{M}^+\text{+H}+2$, 96%). Anal. Calcd. (%) for $\text{C}_{14}\text{H}_8\text{BrFN}_2\text{OS}$: C, 47.88; H, 2.296; N, 7.977; S, 9.131. Found: C, 47.79; H, 2.423; N, 8.287; S, 9.035.

2-Benzamido-6-methylbenzothiazole (compound #8) [21,22]. Yield: 26% mp 214–216°C (No information about melting point in the references). ^1H NMR (DMSO- d_6 , 400 MHz) δ (ppm): 2.45 (s, 3H, CH_3), 7.05–7.62 (m, 6H, H-4, H-5, H-7, H-3', H-4', H-5'), 8.01 (d, $J = 7.2$ Hz, 2H, H-2', H-6'), NH proton was not monitored; ^{13}C NMR (DMSO- d_6 , 100 MHz) δ (ppm): 21.44, 120.15, 121.13, 127.57, 127.95, 128.98, 131.96, 132.08, 133.00, 134.02, 145.56, 158.97, 165.86; ESIMS m/z 269.33 ($\text{M}^+\text{+H}$, 100%). Anal. Calcd. (%) for $\text{C}_{15}\text{H}_{12}\text{N}_2\text{OS} - \text{HOH}$: C, 62.92; H, 4.928; N, 9.783; S, 11.20. Found: C, 63.00; H, 5.072; N, 9.964; S, 11.14.

2-(4'-Bromobenzamido)-6-methylbenzothiazole (compound #9). Yield: 43% mp 259–260°C. ¹H NMR (DMSO-*d*₆, 400 MHz) δ (ppm): 2.42 (s, 3H, CH₃), 7.25 (d, *J* = 8.4 Hz, 1H, H-5), 7.64 (d, *J* = 8.0 Hz, 1H, H-4), 7.75 (d, *J* = 8.8 Hz, 2H, H-3', H-5'), 7.76 (s, 1H, H-7), 8.04 (d, *J* = 8.4 Hz, 2H, H-2', H-6'), 12.89 (s, 1H, NH); ¹³C NMR (DMSO-*d*₆, 100 MHz) δ (ppm): 20.98, 119.80, 121.34, 126.72, 127.53, 130.32, 131.33, 131.63, 133.22; ESIMS *m/z* 347.24 (M⁺+H, 100%), 349.20 (M⁺+H+2, 100%). Anal. Calcd. (%) for C₁₅H₁₁BrN₂OS: C, 51.89; H, 3.193; N, 8.068; S, 9.235. Found: C, 51.82; H, 3.297; N, 8.482; S, 9.239.

2-(4'-Methylbenzamido)-6-methylbenzothiazole (compound #10) [23]. Yield: 47% mp 234–235°C (No information about melting point in the reference). ¹H NMR (DMSO-*d*₆, 400 MHz) δ (ppm): 2.38 (s, 3H, 4'-CH₃), 2.45 (s, 3H, 6-CH₃), 7.08 (d, *J* = 7.6 Hz, 1H, H-5), 7.18–7.26 (m, 3H, H-4, H-3', H-5'), 7.63 (s, 1H, H-7), 7.88 (d, *J* = 8.0 Hz, 2H, H-2', H-6'), NH proton was not monitored; ¹³C NMR (DMSO-*d*₆, 100 MHz) δ (ppm): 21.43, 21.58, 120.25, 121.12, 127.48, 127.89, 129.22, 129.64, 132.05, 133.91, 143.83, 165.67; ESIMS *m/z* 283.35 (M⁺+H, 100%). Anal. Calcd. (%) for C₁₆H₁₄N₂OS: C, 68.06; H, 4.998; N, 9.921; S, 11.36. Found: C, 68.06; H, 4.882; N, 10.16; S, 11.33.

2-(4'-Nitrobenzamido)-6-methylbenzothiazole (compound #11). Yield: 43% mp 278–279°C. ¹H NMR (DMSO-*d*₆, 400 MHz) δ (ppm): 2.42 (s, 3H, CH₃), 7.29 (dd, *J* = 1.2 Hz and *J* = 8.0 Hz, 1H, H-5), 7.65 (d, *J* = 7.6 Hz, 1H, H-4), 7.79 (s, 1H, H-7), 8.31–8.37 (m, 4H, H-2', H-3', H-5', H-6'), 13.14 (s, 1H, NH); ¹³C NMR (DMSO-*d*₆, 100 MHz) δ (ppm): 20.91, 121.42, 123.50, 127.63, 129.78, 133.38, 149.64; ESIMS *m/z* 314.37 (M⁺+H, 100%). Anal. Calcd. (%) for C₁₅H₁₁N₃O₃S: C, 57.5; H, 3.539; N, 13.411; S, 10.23. Found: C, 57.29; H, 3.733; N, 13.55; S, 10.23.

2-(4'-Bromo-*N'*-benzhydrazido)benzothiazole (compound #12) [24]. Yield: 29% mp 235–237°C (No information in the reference). ¹H NMR (DMSO-*d*₆, 400 MHz) δ (ppm): 7.09 (t, *J* = 7.6 Hz, 1H, H-6), 7.27 (t, *J* = 7.2 Hz, 1H, H-5), 7.46 (d, *J* = 7.6 Hz, 1H, H-7), 7.73 (d, *J* = 8.0 Hz, 1H, H-4), 7.75 (d, *J* = 8.4 Hz, 2H, H-3', H-5'), 7.85 (d, *J* = 8.4 Hz, 2H, H-2', H-6'), 10.04 (s, 1H, N'H), 11.04 (s, 1H, NH); ¹³C NMR (DMSO-*d*₆, 100 MHz) δ (ppm): 118.83, 121.28, 121.64, 125.73, 129.44, 130.17, 131.17, 131.65, 152.13, 165.47, 170.16; ESIMS *m/z* 350.22 (M⁺+H, 100%), 348.18 (M⁺+H+2, 95%). Anal. Calcd. (%) for C₁₄H₁₀BrN₃OS – 0.35CH₃OH: C, 57.5; H, 3.539; N, 13.411; S, 10.23. Found: C, 57.29; H, 3.733; N, 13.55; S, 10.23.

Biological assay

In vitro hGSTP1-1 inhibitory activity

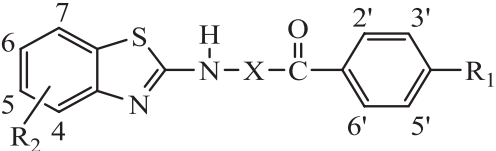
Expression and purification of human GSTP1-1. Recombinant hGSTP1-1 was expressed in *Escherichia coli* strain XL-1 Blue at 37°C and purified by using S-hexylglutathione-Sepharose 6B [25]. *E. coli* XL-1 cells containing pKXHP1 plasmid were grown overnight in 50 ml 2YT media (16 g tryptone, 10 g yeast extract, 5 g NaCl and 100 mg/l ampicillin) and then transferred to 500 ml 2YT media and incubated at 37°C in the shake incubator. Incubation was kept until the absorbance of the culture at 600 nm was 0.2–0.4. Then 0.2 mM isopropyl-β-D-thiogalactopyranoside was added to induce the expression of hGSTP1-1. The cells were further grown for 16 h and then centrifuged at 1500 g for 10 min. The pellets were kept at –80°C for 30 min. The pellets were resuspended in lysis buffer (10 mM Tris HCl, 1 mM Ethylenediamine tetra acetic acid (EDTA), 0.2 mM dithiothreitol (DTT) pH 7.0 and protease inhibitor cocktail, 0.2 mg/ml lysozyme) and mixed gently on ice for 30 min and then disrupted

by sonication 5 times for 20 s. Phenylmethanesulphonyl fluoride (170 μM) was added and the supernatant fraction was obtained by centrifugation at 15,000 g, 4°C for 1 h.

An affinity matrix consisting of S-hexylglutathione immobilized on epoxy-activated-Sepharose 6B was used for purification of hGSTP1-1 [26]. The supernatant fraction was applied to the matrix equilibrated with binding buffer and stirred gently for 40 min on ice. The matrix containing bound hGSTP1-1 was washed with Buffer A (10 mM Tris HCl, pH 7.8, 1 mM EDTA, 0.2 M NaCl, 0.2 mM DTT) to eliminate non-bound proteins. The matrix was packed on top of a Sephadex G-25 column equilibrated with Buffer A in the cold room. The enzyme was then eluted with Buffer B (10 mM Tris HCl, pH 7.8, 1 mM EDTA, 0.2 M NaCl, 0.2 mM DTT, 5 mM S-hexylglutathione). The fractions containing the GST activity were concentrated on ice and then dialysed with Buffer A without NaCl. The purity of the enzyme was validated by SDS-PAGE applying both optimal and excessive protein amounts for analysis to visualize possible impurities.

In vitro hGSTP1-1 inhibition assay. *In vitro* hGSTP1-1 inhibitory activity of the synthesized compounds, which is given in Table 1, was used to measure the initial rate of absorbance change at 340 nm with 1-chloro-2,4-dinitrobenzene (CDNB). Standard enzymatic assay conditions consisted in order of 0.1 M phosphate buffer, pH 6.5 containing 1 mM EDTA, 1 mM GSH, and 1 mM CDNB ($\Delta\epsilon_{340} = 9.6 \text{ mM}^{-1} \text{ cm}^{-1}$) at 30°C [27]. For the inhibition studies, compounds were added just before CDNB and the absorbance change was measured for 1 min in a 1 ml quartz cuvette. The reaction system contained 5% ethanol from CDNB (20 mM stock) and 5% dimethylsulphoxide (DMSO) from the synthesized compounds #1–12 and EA (2 mM stock). Solvents had negligible inhibitory effect on the enzyme activity and the enzymatic reaction was obtained by subtracting the non-enzymatic rate from the rate measured in the presence of enzyme.

Table 1. Structures and the observed IC_{50} values of the synthesized benzothiazole derivatives for hGSTP1-1.



Comp. No	X	Substituents		hGSTP1-1 IC_{50} (μM)
		R_1	R_2	
—	—	H	H	>100
—	—	Br	H	12†
—	—	CH_3	H	30
—	—	NO_2	H	ND
*	—	Br	4- CH_3	15.1†
*	—	NO_2	4- CH_3	ND
*	—	Br	6-F	30
—	—	H	6- CH_3	>100
*	—	Br	6- CH_3	38.9
—	—	CH_3	6- CH_3	30
*	—	NO_2	6- CH_3	ND
—	NH	Br	H	>100
Ethacrynic acid				10.2

*Compounds, which are original.

†Most active compounds.

ND, Not Detected, due to their solubility problems.

Data analysis. All activity measurements were made in triplicate of three different concentrations of synthesized compounds. The IC_{50} value represents the concentration of the inhibitor that gives 50% inhibition of the enzymatic activity. These IC_{50} values of the compounds were determined by regression analysis using Graphpad Prism 4.0 software [28].

Molecular modelling

Pharmacophore analysis (HipHop method)

The HipHop method was used to generate pharmacophore hypotheses to explain the specification of the structure–activity relationships of pharmacophoric sites of the lead compounds [29–33]. Molecules were built using the DS 3.5. software and standard 3D structures were generated and the geometry of all molecules was optimized with Adopted Basis Newton Rapson (ABNR) Minimization Method and conformational models for each compound were automatically generated. The ‘best conformer generation’ procedure was applied to provide the best conformational coverage for a maximum number of conformers generated, defaulted to 255 in a 0–20 kcal/mol range from the global minimum. The generated conformations were used to align common molecular features and generate a pharmacophore hypothesis. According to the activity results, the HipHop method was applied to build the pharmacophore model and the hypothesis was generated by using the active ligand structures as the ‘reference compounds’ [34–36].

For the generation of the HipHop pharmacophore process, a set of six active compounds (Compounds #2, 3, 5, 7, 9 and 10) in Table 1 were selected as the target training set. Among the selected molecules, the most active molecules, compounds #2 and #5, were chosen as the ‘reference compounds’, specifying a principal value of 2 and a maximum omitting features (MaxOmitFeat) value of 0, as given in Table 2. Ten pharmacophoric hypotheses were generated from these aligned structures using the Common Feature Pharmacophore Generation protocol (Table 3). A preparative test was performed with hydrogen bond acceptor (HBA),

Table 2. The characteristics of the compounds used in the training set and the chosen reference compounds for the generation of the pharmacophore hypotheses, together with the test set compounds, which were mapped to the generated model.

Comp.	FitValue	Principal ^c	MaxOmitFeat ^d	HpAr-1 ^e	HpAr-2 ^f	Hp ^g	HBA ^h	Pharmprint
1 ^b	1.99	0	2	1	1	1	1	'1111'
2 ^{*a}	3.99	2	0	1	1	1	1	'1111'
3 ^a	3.94	1	2	1	1	1	1	'1111'
5 ^{*a}	3.99	2	0	1	1	1	1	'1111'
7 ^a	3.98	1	2	1	1	1	1	'1111'
8 ^b	1.86	0	2	1	1	1	1	'1111'
9 ^a	3.93	1	2	1	1	1	1	'1111'
10 ^a	3.87	1	2	1	1	1	1	'1111'
12 ^b	1.90	0	2	1	1	1	1	'1111'

*Reference compounds; ^aTraining set compounds.

^bTest set compounds.

^cPrincipal: 1 = molecule must map onto the hypotheses generated by the search procedure. Partial mapping is allowed. 2 = reference compound. The chemical feature space of the conformers of such a compound is used to define the initial set of potential hypotheses.

^dThe MaxOmitFeat column specifies how many hypotheses map all features, a 2 shows hypotheses to which no compound feature maps.

^eHydrophobic aromatic feature of the thiazole ring in the fused ring system.

^fHydrophobic aromatic feature of the benzene ring in the fused ring system.

^gHydrophobic feature of the substituent on the 4th position of the phenyl ring.

^hHydrogen bond acceptor feature of carbonyl oxygen in the amide function substituted on the 2nd position at the benzo-thiazole ring system.

Table 3. Rank scores of the 10 generated hypotheses.

	Features ^a	Rank	Direct Hit ^b	Partial Hit ^b	Max Fit
01	YYHA	74.376	1111111	0000000	4
02	RZAA	72.949	1111111	0000000	4
03	YYHA	71.890	1111111	0000000	4
04	RYHA	70.385	1111111	0000000	4
05	RYHA	70.385	1111111	0000000	4
06	YZAA	70.135	1111111	0000000	4
07	YYZA	69.999	1110111	0001000	4
08	RYZA	69.610	1110111	0001000	4
09	RYZA	69.610	1110111	0001000	4
10	RYZA	69.599	1110111	0001000	4

^aA = Hydrogen Bond Acceptor Feature; H = Hydrophobic Feature; R = Ring Aromatic Feature; Y = Hydrophobic Aromatic Feature; Z = Hydrophobic Aliphatic Feature.

^bDirect hit, all the features of the hypothesis are mapped. Direct Hit = 1 means yes; Partial Hit, partial mapping of the hypothesis. Partial Hit = 0 means no. Each number refers to molecules where MaxOmitFeat is 0 (same order).

hydrogen bond donor (HBD), hydrophobic aromatic (HpAr), hydrophobic aliphatic (HpAl), hydrophobic (Hp), and ring aromatic (R). The first hypothesis, shown in Figure 2a, which possessed the highest ranking score (74.376), given in Table 3, has been chosen for the anticipated model among the other generated potential hypotheses. The fit values of the training set compounds (#2, 3, 5, 7, 9 and 10) observed from the 1st hypothesis are shown in Table 2.

Docking (CDocker method)

Docking is an effective method to predict ligands, which are small molecules that may interact with a macromolecular target such as an enzyme [37,38].

The crystal structure of the hGSTP1-1, complexed with GSH, was extracted from the Protein Data Bank (pdb ID: 2GSS) [39]. DS 3.5 software was used for the preparation of protein and ligands [16]. Crystal structure of hGSTP1-1 was taken from the pdb ID: 2GSS, hydrogens were added and optimized using the all atom CHARMM forcefield and the ABNR method until the root mean square (RMS) gradient was < 0.05 kcal/mol/Å². The minimized protein was defined as the receptor using the binding site module. The binding site was defined from the cavity finding method and modified to contain all of the important active site residues in the H site of the enzyme. Binding sphere was selected from the active site using the binding site tools (6.64, 3.67, 26.88, 9.312). Novel synthesized benzothiazole derivatives and the reference drug (EA) were sketched, all atom CHARMM forcefield parameterization was assigned and minimized as described above. Conformational searches of the ligands were carried out using a simulated annealing molecular dynamics (MD) approach. The ligands were heated to a temperature of 700 K and then annealed to 200 K. CDocker method was performed by using DS 3.5 [40]. The hGSTP1-1 enzyme was held rigid, while the ligands were allowed to be flexible during refinement. The docking and scoring methodology was first validated by docking of EA. The docked position of EA overlaps well with the crystal structure position, with an RMSD of 0.677 Å. Molecular docking studies were performed and all docked poses were scored by applying the Analyse Ligand Poses sub-protocol. Binding energies were calculated by using *in situ* ligand minimization step (ABNR Method) and using implicit solvent model [Generalized Born Molecular Volume (GBMV)] in DS 3.5. The lowest binding energies were taken as the best-docked conformation of the compound to the macromolecule. The pictures were taken by using DS 4.5 Visualizer.

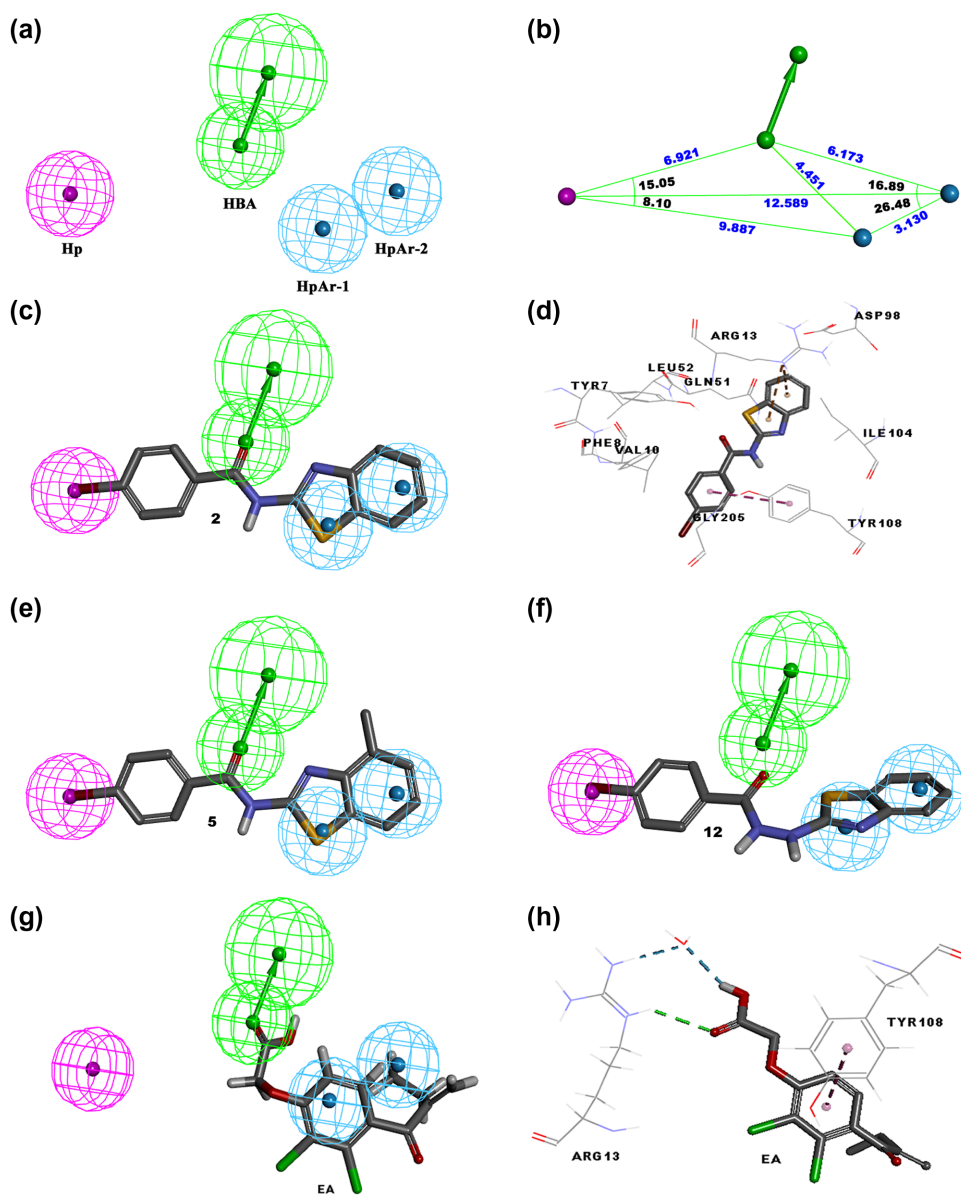


Figure 2. (a) Anticipated pharmacophore model generated for hGSTP1-1 inhibitor activity of tested compounds [Hydrophobic (Hp) feature, magenta; Hydrogen Bond Acceptor (HBA) feature, green; Hydrophobic Aromatic (HpAr) feature, blue]. (b) Distances (Å, blue) and angles (°, black) between the generated common features calculated in the participated pharmacophore model. (c) Pharmacophore mapping of most active tested lead compound #2. (d) Docking pose of the most active tested lead compound #2: phenyl group revealed π - π interaction with Tyr108 and benzothiazole ring revealed two π -cation interactions with Arg13. (e) Pharmacophore mapping of tested active compound #5. (f) Pharmacophore mapping of tested non-active compound #12. (g) Pharmacophore mapping of Ethacrynic acid (EA). (h) Docking pose of EA: carboxyl group revealed H bond with Arg13 (2.76 Å) and H₂O (2.53 Å), compound had interactions with Tyr108 (π - π). * All of the ligands are seen as stick representations, H bonds are shown as green dashed lines, and other interactions are shown as magenta dashed lines.

Results and discussion

In this study, 12 benzothiazole derivatives were synthesized (compounds #1–12), of which five of them (compounds #5–7, 9 and 11) were novel (Table 1). The syntheses of the compounds # 1–12 were performed by using the microwave apparatus.

Biological assay

The nine synthesized compounds (#1–3, 5, 7–10 and 12) were tested with *in vitro* IC_{50} inhibitory activities on hGSTP1-1 enzyme. The remaining three compounds (#4, 6 and 11) could not be tested due to their solubility problems. EA was used as the reference drug. The observed *in vitro* hGSTP1-1 enzyme inhibitor activities of the synthesized compounds and reference drug in the manner of IC_{50} values (μM) are given in Table 1. Whereas some of the tested compounds (#2, 3, 5, 7, 9 and 10) showed IC_{50} values between 12–38.9 μM , other compounds (#1, 8 and 12) exhibited an inhibitory response of more than 100 μM . However, the *in vitro* inhibitory activity of the synthesized compounds #4, 6 and 11 could not be detected because of their solubility problems. Hereby, two compounds (#2 and #5) were found to be lead compounds, exhibiting significant hGSTP1-1 enzyme inhibitory activities. Especially, compound #2 showed an inhibition similar to EA with 12 μM values. According to the structure–activity relationships analysis, bromine substitution at R_1 position increased the activity. On the other hand, any substitution on the benzothiazole ring was found to decrease the activity. Moreover, methyl substitution at the 4th position of the fused heterocyclic ring system, methyl or fluorine substitutions at the 6th position and holding a hydrazine bridge instead of amine group at the 2nd position were also revealed to decrease the inhibitory activity.

Molecular modelling

In order to describe the binding site features of the most active lead benzothiazoles among the tested compounds on hGSTP1-1 enzyme, the HipHop pharmacophore generation method and molecular docking (CDocker method) studies were performed by using DS 3.5 software. The HipHop method was used to generate pharmacophore hypotheses to explain the specification of the structure–activity relationships of pharmacophoric sites of the tested compounds. The HipHop pharmacophore model was generated with a set of six active compounds used as the training set (compounds #2, 3, 5, 7, 9 and 10) and the most active compounds (#2 and 5) were selected as the reference compounds. Within the 10 generated hypotheses given in Table 3, the first hypothesis (shown in Figure 2(a)), which possessed the highest rank value, was chosen as the anticipated model. The fit values of the training set compounds (#2, 3, 5, 7, 9 and 10) are shown in Table 2. The mapping of the synthesized inactive benzothiazole derivatives were chosen for test set (#1, 8 and 12) and their observed fit values were found to be 1.99, 1.86 and 1.90, respectively, which were displayed as fitting less to the anticipated model compared to the active ones (Table 2). The example of the mapping of compound 12 with the generated pharmacophore model features is given in Figure 2(f).

The generated pharmacophore model given in Figure 2(a) revealed that the hydrophobic feature on R₁ position at the 2-substituted phenyl ring, especially holding a deactivating group like bromine is important for the hGSTP1-1 enzyme inhibitory activity. As shown in the performed docking results (Figure 2(d)), the most active compound (#2) has a π - π interaction with the protein active site residual Tyr108.

Looking at the mapped structure of the lead compound (#2) with the anticipated hypothesis, pharmacophoric features (Figure 2(c)) were well correlated with the performed docking results. As shown in the anticipated pharmacophore model, the hydrophobic feature seemed to be on the substituent at the 4th position of the phenyl ring and compound revealed a π - π interaction with Tyr108 over the phenyl ring. The hydroxyl group in the phenyl ring of Tyr108 increased the electron density on the ring in view of the fact that free electrons of the oxygen activated the phenyl ring of Thy108, acting as an electron donor. In contrast, the bromine group in the phenyl ring at compound #2 reduced the electron density and deactivated the phenyl ring by means of strong electronegative properties of halogens and the compound could reveal a π - π interaction with Tyr108 by acting like an electron acceptor. The presence of substituents which deactivate the ring more than bromine may cause a stronger interaction and, thus, increases the inhibitory activity.

In the generated pharmacophore hypothesis, the hydrophobic aromatic feature at the benzothiazole fused ring system was observed as significant. Appropriate to this finding, the monitored molecular docking pose also revealed that the most active lead compound (#2) possessed a π -cation interaction with Arg13 *via* this fused ring system. In respect of these findings, structure-activity relationships indicate that methyl substitution on the 4th or 6th position of the benzothiazole fused ring system cause reductions in the inhibitory activity. The reason for this decrease was thought to be due to the field effect of the methyl group. It was predicted that the methyl group on the 4th or 6th position of the benzothiazole ring attracted the free electrons participating in the resonance by reducing the electron density on the sulphur and reduced the aromatization by reducing electron density at *meta* position, neighbouring sulphur in the thiazole ring. Hereby, as the aromaticity on the benzothiazole ring decreased, the inhibitor activity also decreased. On behalf of these findings, we can predict that the presence of groups that activate the benzothiazole fused ring system on the 5th or 7th positions increases the hydrophobic aromaticity due to the direct contribution to the aromatization without reducing the resonance provided by the sulphur atom in the thiazole ring, then the interaction between the residuals at the active side of the protein could be stronger, causing an increase in the inhibitor activity.

According to the performed docking results given in Figure 2(d), the most active compound (#2) revealed a π - π interaction with the active side residual Tyr108 and two π -cation interactions with Arg13 (Figure 2(d)). The calculated docking pose binding energy value of compound #2 was found to be -16.3635 kcal/mol, showing significant binding interaction with the H side active residuals of the hGSTP1-1. The well-known ligand EA revealed a H bond with Arg13 (2.27 Å) and a π - π interaction with Tyr108 (Figure 2(h)). The calculated binding energy was -21.539 kcal/mol.

The docking study was corroborated, owing to the fact that compound #2 showed binding interactions with the same amino acid residuals as EA with Try108 and Arg13, but showed a different type of bonding with Arg13. While EA bound with a H-bond (acting as a HBA), compound #2 formed a π -cation interaction with this active site residue. There is a different

chemical bond type between EA and compound #2 while binding Arg13, with EA bound *via* H-bond to Arg13, causing a stronger binding energy score than compound #2.

Furthermore, when EA mapped to the generated pharmacophore model, because of the different chemical bonding type while binding to Arg13, EA displayed a map that was not fitted to the magenta coloured hydrophobic (Hp) feature side. However, if the docking poses of EA and the active compound #2 for the binding interactions with the active site residuals are compared, it was displayed that this hydrophobic (Hp) pharmacophoric feature side was important for the active benzothiazole compound #2 bound *via* Arg13, which is not the same for EA (Figures 2D2(d) and (h)). These findings revealed that EA and the synthesized benzothiazole compounds comprised different features of the anticipated pharmacophore model with the different binding interactions via the active site residuals. While the lead compound (#2) displayed pharmacophoric features as HpAr-1, HpAr-2 and Hp, EA revealed the pharmacophoric features as HpAr-1, HpAr-2 and HBA at the anticipated pharmacophore model for the inhibitory activity of the hGSTP1-1. Consequently, these observations demonstrated that cooperative usage of the pharmacophore model and docking study further enlightens the understanding of the binding interactions of different substrates of the same active site.

Conclusion

The synthesized substituted benzothiazoles are estimated to possess an inhibitory activity on the hGSTP1-1 by binding to the H-site as a substrate according to the results of molecular modelling studies.

The synthesized substituted benzothiazoles structure–activity relationships analysis revealed that the *para* position of the phenyl ring of the benzamide moiety substituted to the 2nd position to the benzothiazole ring is found to be important and substitution of this position with a hydrophobic atom and/or atom groups that reduced the electron density at the phenyl ring is required for the π – π interaction with the H side active residue Tyr 108 of the hGSTP1-1.

Moreover, the hydrophobic aromatic property of the benzothiazole fused ring system was also found to be important and the rich electron density property for the benzothiazole ring was highly required to have an interaction with the H side cationic nitrogen atom of Arg 13.

In conclusion, compounds #2 and #5 could be used as scaffolds in the drug design studies of new potent hGSTP1-1 inhibitors in cancer chemotherapy. It is planned to achieve more active lead compounds as hGSTP1-1 inhibitors by generating chemical modifications through these compounds and applying new regulations so as to increase the water solubility of existing compounds to overcome their solubility problem.

Acknowledgements

This work was supported by the Swedish Cancer Society and the Swedish Research Council.

Disclosure statement

No potential conflict of interest was reported by the authors.

References

- [1] K.D. Tew, *Glutathione-associated enzymes in anticancer drug resistance*, *Cancer Res.* 54 (1994), pp. 4313–4320.
- [2] J.D. Hayes, J.U. Flanagan, and I.R. Jowsey, *Glutathione transferases*, *Annu. Rev. Pharmacol. Toxicol.* 45 (2005), pp. 51–88.
- [3] T.W. Schultz, J.W. Yarbrough, and E.L. Johnson, *Structure-activity relationships for reactivity of carbonyl-containing compounds with glutathione*, *SAR QSAR Environ. Res.* 16 (2005), pp. 313–322.
- [4] P.D. Josephy and B. Mannervik, *Molecular Toxicology*, 2nd ed., Oxford University Press, New York, 2006.
- [5] N. Mathew, M. Kalyanasundaram, and K. Balaraman, *Glutathione S-transferase (GST) inhibitors*, *Expert Opin. Ther. Patents* 16 (2006), pp. 431–444.
- [6] J.A. Schwobel, J.C. Madden, and M.T. Cronin, *Examination of Michael addition reactivity towards glutathione by transition-state calculations*, *SAR QSAR Environ. Res.* 21 (2010), pp. 693–710.
- [7] N. Ban, Y. Takahashi, T. Takayama, T. Kura, T. Katahira, S. Sakamaki, and Y. Niitsu, *Transfection of glutathione S-transferase (GST)-pi antisense complementary DNA increases the sensitivity of a colon cancer cell line to adriamycin, cisplatin, melphalan, and etoposide*, *Cancer Res.* 56 (1996), pp. 3577–3582.
- [8] C.S. Morrow, P.K. Smitherman, S.K. Diah, E. Schneider, and A.J. Townsend, *Coordinated action of glutathione S-transferases (GSTs) and multidrug resistance protein 1 (MRP1) in antineoplastic drug detoxification. Mechanism of GST A1-1- and MRP1-associated resistance to chlorambucil in MCF7 breast carcinoma cells*, *J. Biol. Chem.* 273 (1998), pp. 20114–20120.
- [9] V. Adler, Z. Yin, S.Y. Fuchs, M. Benezra, L. Rosario, K.D. Tew, M.R. Pincus, M. Sardana, C.J. Henderson, C.R. Wolf, R.J. Davis, and Z. Ronai, *Regulation of JNK signaling by GSTp*, *EMBO J.* 18 (1999), pp. 1321–1334.
- [10] T. Asakura, A. Sasagawa, H. Takeuchi, S. Shibata, H. Marushima, S. Mamori, and K. Ohkawa, *Conformational change in the active center region of GST P1–1, due to binding of a synthetic conjugate of DXR with GSH, enhanced JNK-mediated apoptosis*, *Apoptosis* 12 (2007), pp. 1269–1280.
- [11] T.P. Mulder, W.H. Peters, T. Wobbles, B.J. Witteman, and J.B. Jansen, *Measurement of glutathione S-transferase P1–1 in plasma: Pitfalls and significance of screening and follow-up of patients with gastrointestinal carcinoma*, *Cancer* 80 (1997), pp. 873–880.
- [12] A.J. Oakley, M. Lo Bello, A. Battistoni, G. Ricci, J. Rossjohn, H.O. Villar, and M.W. Parker, *The structures of human glutathione transferase P1–1 in complex with glutathione and various inhibitors at high resolution*, *J. Mol. Biol.* 274 (1997), pp. 84–100.
- [13] T. Ertan-Bolelli, Y. Musdal, K. Bolelli, S. Yilmaz, Y. Aksoy, I. Yildiz, E. Aki-Yalcin, and I. Yalcin, *Synthesis and biological evaluation of 2-substituted-5-(4-nitrophenylsulfonamido)benzoxazoles as human GST P1–1 inhibitors, and description of the binding site features*, *ChemMedChem* 9 (2014), pp. 984–992.
- [14] T. Ertan-Bolelli, K. Bolelli, Y. Musdal, I. Yildiz, E. Aki-Yalcin, B. Mannervik, and I. Yalcin, *Design and synthesis of 2-substituted-5-(4-trifluoromethylphenyl-sulphonamido)benzoxazole derivatives as human GST P1–1 inhibitors*, *Artif. Cells Nanomed, Biotechnol.* (2017), pp. 1–8 In press. Doi: <https://doi.org/10.1080/21691401.2017.1324464>.
- [15] Y. Musdal, T. Ertan-Bolelli, K. Bolelli, S. Yilmaz, D. Ceyhan, U. Hegazy, B. Mannervik, and Y. Aksoy, *Inhibition of human glutathione transferase P1–1 by novel benzazole derivatives*, *Turk. J. Biochem.* 37 (2012), pp. 431–436.
- [16] Dassault Systemes BIOVIA, *Discovery Studio 3.5*, Dassault Systèmes, San Diego, CA, 2012.
- [17] I. Yalcin, B.K. Kaymakcioglu, I. Oren, E. Sener, O. Temiz, A. Akin, and N. Altanlar, *Synthesis and microbiological activity of some novel N-(2-hydroxyl-5-substitutedphenyl)benzacetamides, phenoxyacetamides and thiophenoxyacetamides as the possible metabolites of antimicrobial active benzoxazoles*, *Farmaco* 52 (1997), pp. 685–689.
- [18] J. Angulo-Cornejo, M. Lino-Pacheco, R. Richter, L. Hennig, K.H. Hallmeier, and L. Beyer, *Metal chelates of N-benzothiazol-2-yl-, N-benzoxazol-2-yl- and N-(1H-benzimidazol-2-yl)-benzamide*, *Inorg. Chim. Acta* 305 (2000), pp. 38–45.
- [19] U.V. Ramesh, R. Singh, D.G. Payan, F. Parlati, R. Lowe, and G.C. Look, *Benzothiazole compositions and their use as ubiquitin ligase inhibitors*, US Patent, 2005, US 2005/0130974 A1.

- [20] T.R. Bailey and D.C. Pevear, *Benzothiazole compounds, compositions and methods for treatment and prophylaxis of rotavirus infections and associated diseases*, Int. Patent, 2004, WO 2004/078115 A2.
- [21] P. Spurr, *Cyclization process for substituted benzothiazole derivatives*, US Patent, Switzerland, 2004, US 2004/0138465 A1.
- [22] G.D. Shen, X. Lv, and W.L. Bao, *Synthesis of N-substituted-2-aminobenzothiazoles by ligand-free copper(I)-catalyzed cross-coupling reaction of 2-haloanilines with isothiocyanates*, Eur. J. Org. Chem. (2009), pp. 5897–5901.
- [23] Y. Hur, D.-H. Kim, E.-K. Kim, J.-H. Park, J.-E. Joo, H.-W. Kang, S.-W. Oh, D.-K. Kim, and K.-K. Ahn, *Phenylimide-containing benzothiazole derivative or its salt and pharmaceutical composition comprising the same*, Int. Patent, 2013, WO 2013/043001 A1.
- [24] R.N. Butler, P. O'Sullivan, and F.L. Scott, *The reactions of lead tetra-acetate with substituted benzothiazolylhydrazones*, J. Chem. Soc. C (1971), pp. 2265–2268.
- [25] R.H. Kolm, G. Stenberg, M. Widersten, and B. Mannervik, *High-level bacterial expression of human glutathione transferase P1–1 encoded by semisynthetic DNA*, Protein Expression Purif. 6 (1995), pp. 265–271.
- [26] B. Mannervik and C. Guthenberg, *Glutathione transferase (human placenta)*, Methods Enzymol. 77 (1981), pp. 231–235.
- [27] W.H. Habig, M.J. Pabst, and W.B. Jakoby, *Glutathione S-transferases. The first enzymatic step in mercapturic acid formation*, J. Biol. Chem. 249 (1974), pp. 7130–7139.
- [28] *Graphpad Prism 4.0*, Graphpad Software, Inc., La Jolla, CA, 2010.
- [29] H. Yuan, H. Liu, W. Tai, F. Wang, Y. Zhang, S. Yao, T. Ran, S. Lu, Z. Ke, X. Xiong, J. Xu, Y. Chen, and T. Lu, *Molecular modelling on small molecular CDK2 inhibitors: An integrated approach using a combination of molecular docking, 3D-QSAR and pharmacophore modelling*, SAR QSAR Environ. Res. 24 (2013), pp. 795–817.
- [30] S. Yilmaz, G. Altinkanat-Gelmez, K. Bolelli, D. Gunecer-Merdan, M.U. Over-Hasdemir, I. Yildiz, E. Aki-Yalcin, and I. Yalcin, *Pharmacophore generation of 2-substituted benzothiazoles as AdeABC efflux pump inhibitors in A. baumannii*, SAR QSAR Environ. Res. 25 (2014), pp. 551–563.
- [31] S. Yilmaz, G. Altinkanat-Gelmez, K. Bolelli, D. Gunecer-Merdan, M. Ufuk Over-Hasdemir, E. Aki-Yalcin, and I. Yalcin, *Binding site feature description of 2-substituted benzothiazoles as potential AcrAB-TolC efflux pump inhibitors in E. coli*, SAR QSAR Environ. Res. 26 (2015), pp. 853–871.
- [32] S.S. Bhayye, K. Roy, and A. Saha, *Pharmacophore generation, atom-based 3D-QSAR, HQSAR and activity cliff analyses of benzothiazine and deaxanthine derivatives as dual A2A antagonists/MAOB inhibitors*, SAR QSAR Environ. Res. 27 (2016), pp. 183–202.
- [33] A. Ozalp, S.C. Yavuz, N. Sabanci, F. Copur, Z. Kokbudak, and E. Saripinar, *4D-QSAR investigation and pharmacophore identification of pyrrolo[2,1-c][1,4]benzodiazepines using electron conformational-genetic algorithm method*, SAR QSAR Environ. Res. 27 (2016), pp. 317–342.
- [34] A. Smellie, S.L. Teig, and P. Towbin, *Poling: Promoting conformational variation*, J. Comput. Chem. 16 (1995), pp. 171–187.
- [35] E.M. Krovat, K.H. Fruhwirth, and T. Langer, *Pharmacophore identification, in silico screening, and virtual library design for inhibitors of the human factor Xa*, J. Chem. Inf. Model. 45 (2005), pp. 146–159.
- [36] I. Yildiz, T. Ertan, K. Bolelli, O. Temiz-Arpaci, I. Yalcin, and E. Aki, *QSAR and pharmacophore analysis on amides against drug-resistant S. aureus*, SAR QSAR Environ. Res. 19 (2008), pp. 101–113.
- [37] A.N. Hidayat, E. Aki-Yalcin, M. Beksac, E. Tian, S.Z. Usmani, T. Ertan-Bolelli, and I. Yalcin, *Insight into human protease activated receptor-1 as anticancer target by molecular modelling*, SAR QSAR Environ. Res. 26 (2015), pp. 795–807.
- [38] E. Aki-Yalcin, T. Ertan-Bolelli, T. Taskin-Tok, O. Ozturk, S. Ataei, C. Ozen, I. Yildiz, and I. Yalcin, *Evaluation of inhibitory effects of benzothiazole and 3-amino-benzothiazolium derivatives on DNA topoisomerase II by molecular modeling studies*, SAR QSAR Environ. Res. 25 (2014), pp. 637–649.
- [39] A.J. Oakley, J. Rossjohn, M. Lo Bello, A.M. Caccuri, G. Federici, and M.W. Parker, *The three-dimensional structure of the human Pi class glutathione transferase P1–1 in complex with the inhibitor ethacrynic acid and its glutathione conjugate*, Biochemistry 36 (1997), pp. 576–585.
- [40] G.S. Wu, D.H. Robertson, C.L. Brooks, and M. Vieth, *Detailed analysis of grid-based molecular docking: A case study of CDOCKER - A CHARMM-based MD docking algorithm*, J. Comput. Chem. 24 (2003), pp. 1549–1562.